Rotational structures and their evolution with spin in ^{152}Gd

D. B. Campbell,[1] R. W. Laird,[2] M. A. Riley,[3] J. Simpson,[4] F. G. Kondev,[5,6] D. J. Hartley,[7] R. V. F. Janssens,[5] T. B. Brown,[8] M. P. Carpenter,[5] P. Fallon,[9] S. M. Fischer,[10] T. Lauritsen,[5] D. Nisius,[5] and I. Ragnarsson[11]

[1]*Lawrence Livermore National Laboratory, Livermore, California 94551, USA*
[2]*Department of Physics, Texas Lutheran University, Seguin, Texas 78023, USA*
[3]*Department of Physics, Florida State University, Tallahassee, Florida 32306, USA*
[4]*CCLRC Daresbury Laboratory, Daresbury, Warrington, WA4 4AD, United Kingdom*
[5]*Physics Division, Argonne National Laboratory, Argonne, Illinois 60439, USA*
[6]*Nuclear Engineering Division, Argonne National Laboratory, Argonne, Illinois 60439, USA*
[7]*Department of Physics, United States Naval Academy, Annapolis, Maryland 21402, USA*
[8]*Savannah River National Laboratory, Aiken, South Carolina 29802, USA*
[9]*Nuclear Science Division, Lawrence Berkeley National Laboratory, Berkeley, California 94720, USA*
[10]*Department of Physics, DePaul University, Chicago, Illinois 60614-3504, USA*
[11]*Division of Mathematical Physics, LTH, Lund University, Box 118, S-221 00, Lund, Sweden*

(Received 8 February 2007; published 19 June 2007)

The fusion-evaporation reaction involving a 175 MeV ^{36}S beam and a ^{124}Sn target was performed, and the emitted γ rays were observed with the Gammasphere spectrometer. Significant additions to the level scheme of ^{152}Gd were made in spite of the relative weakness of the α4n exit channel, being only $\sim$2% of the total fusion cross-section. The high-spin behavior of ^{152}Gd was compared with that of other $N = 88$ nuclei. A striking similarity was observed with ^{154}Dy and it is therefore suggested that the angular-momentum-induced shape changes that take place in ^{154}Dy also occur in ^{152}Gd in the 30–40$\hbar$ spin range. This is supported by Cranked Nilsson-Strutinsky calculations which were used to interpret the high-spin bands. It is found that a better agreement between calculation and experiment is obtained if the $Z = 64$ shell gap increases with a decreasing number of valence particles outside the doubly-closed $^{146}_{64}Gd_{82}$ nucleus.

DOI: 10.1103/PhysRevC.75.064314 PACS number(s): 27.70.+q, 21.10.Re, 23.20.Lv

I. INTRODUCTION

The light rare-earth region is well known for its transitional nature, beautifully illustrated by the differences exhibited between the $N \leqslant 88$ and $N \geqslant 90$ isotones [1,2] where the addition of just a few neutrons accounts for a dramatic shift from a vibrational to a rotational character. Gadolinium isotopes are at the center of this transitional region; however, it is difficult to study the high-spin structure of these key nuclei, including ^{152}Gd, due to the difficulty of producing them with available stable beam/target combinations. One fruitful approach to studying these nuclei [3] is to investigate weak exit channels, such as αxn, from reactions utilizing stable beams and targets. In the current work, new insight is possible in these channels due to the considerable resolving power of the highly efficient γ-ray detector system employed, namely Gammasphere [4].

II. EXPERIMENTAL DETAILS

An experiment primarily focused on the ultra-high-spin ($I \approx 60\hbar$) characteristics of ^{156}Dy [5] was conducted at Lawrence Berkeley National Laboratory. A 175 MeV ^{36}S beam, obtained from the 88" Cyclotron, induced fusion-evaporation reactions with two stacked 400 μg/cm^2 ^{124}Sn targets. The resulting γ rays were detected with the Gammasphere spectrometer, which contained 93 high purity Ge detectors at the time of the measurement. A total of 1.3×10^9 events were collected when at least five Compton-suppressed Ge detectors fired in prompt coincidence. Analysis of ^{152}Gd was performed using triple-coincidence (γ^3) RADWARE [6] cubes containing known transitions (e.g. $2^+ \rightarrow 0^+$, $4^+ \rightarrow 2^+$) in ^{152}Gd, as well as a four-dimensional (γ^4) RADWARE hypercube, constructed from a Blue [7] database

The α4n channel leading to ^{152}Gd constituted less than 2% of the total fusion cross-section. It was still possible, however, to significantly expand the ^{152}Gd level scheme. Transitions are positioned in the scheme based on intensity arguments and coincidence relationships. Spin assignments for key interband transitions were verified using a version of the Directional Correlations from Oriented states (DCO) [8–10] procedure. All other in-band transitions are assumed to be of stretched quadrupole character.

III. EXPERIMENTAL RESULTS

The current level scheme for ^{152}Gd is shown in Fig. 1 where we have made several rearrangements and reassignments to the previous level schemes presented in Refs. [11,12] and significant extensions to the level scheme presented in Ref. [13]. For positive parity bands, three transitions were added to Band 1, the ground state band, pushing the maximum observed spin from 20$\hbar$ [12] to 26$\hbar$. Transitions in Band 1 above the previous limit were marked by reduced intensity as Band 7 becomes yrast at 18$\hbar$. The 696-keV interband γ ray was the most intense transition from Band 7, feeding into

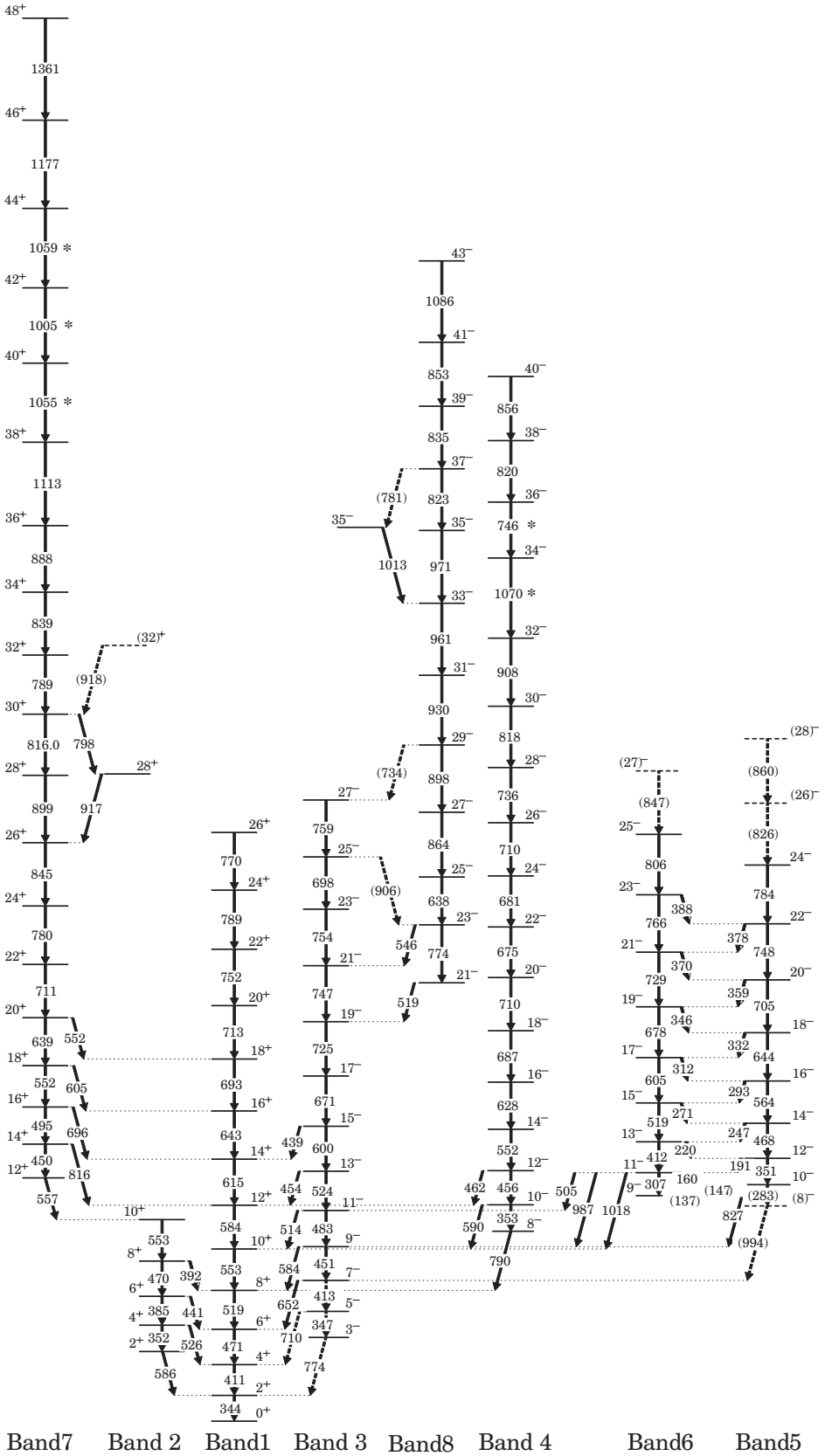

FIG. 1. The level scheme for ^{152}Gd deduced in this work. The "*" symbols denote γ rays whose exact order in the sequence cannot be firmly established. Tentatively placed γ rays are depicted with dashed lines.

Band 1 ($16^+ \rightarrow 14^+$). Band 7 was observed to spin $48\hbar$; however, the precise ordering of some of the γ rays is uncertain near the top, as denoted in Fig. 1. The uncertainty in ordering does not change the main conclusions of this work. Band 2 was originally reported to $10\hbar$ [11]. Recent extensions to Band 2 reported by Ref. [12] have been assigned to Band 7 in the current work, and Ref. [13]. Band 3 was previously reported to a spin of $21\hbar$ [12] and Band 4 was known up to the 710-keV transition [13].

With regard to the negative parity bands in the current ^{152}Gd level scheme, Band 8 is entirely new, while bands 3, 4, 5 and 6 were considerably extended. Band 3 was extended from $21\hbar$ [12,13] to $27\hbar$. Similarly, Band 4 was extended by 10 transitions from the previous maximum of $20\hbar$ [13]. Band 4 was originally reported as tentatively having positive parity with odd spin values [11,12] whereas the current level scheme and Ref. [13] interpret Band 4 as being of negative parity with even spin, see discussion below.

The strongly coupled bands 5 and 6, previously reported to $16\hbar$ and $17\hbar$ [13], are tentatively observed to spins of $28\hbar$ and $27\hbar$ respectively, as in Fig. 1. The bulk of intensity for these bands flows out through the 1018- and 827-keV transitions into the ground state band 10^+ level. The examination of this structure was particularly challenging as many of the E2 transitions are similar in energy to large peaks from major reaction channels, such as ^{154}Dy. However, the dipole transitions were sufficiently strong to allow the determination of their high-spin counterparts. Unfortunately, the feed-out transitions from these bands proved too weak to obtain DCO ratios. Consequently, spin assignments were based primarily on the 11^- level that feeds both a 9^- state and an 11^- state via the 505- and 987-keV transitions. These assignments are supported by additional linking transitions reported in Ref. [13].

Band 8 is new and was observed to the highest spin in a ^{152}Gd negative parity band: $43\hbar$, as in Fig. 1. Band 8 contains the lowest energy 21^- state yet observed in ^{152}Gd, with the bulk of intensity flowing to Band 3 through the 519-keV transition. Other linking γ rays were observed, and spin values for the band were assigned based on these transitions. In addition, the 1013-keV transition which feeds into Band 8 at $33\hbar$ suggests it undergoes a band crossing at $35\hbar$.

Representative spectra for bands 4, 5, 6, 7 and 8 are shown in Fig. 2. These spectra were generated through triple coincidence gates on a four-fold hypercube using the key transitions denoted with "#" symbols in the spectra. Selective

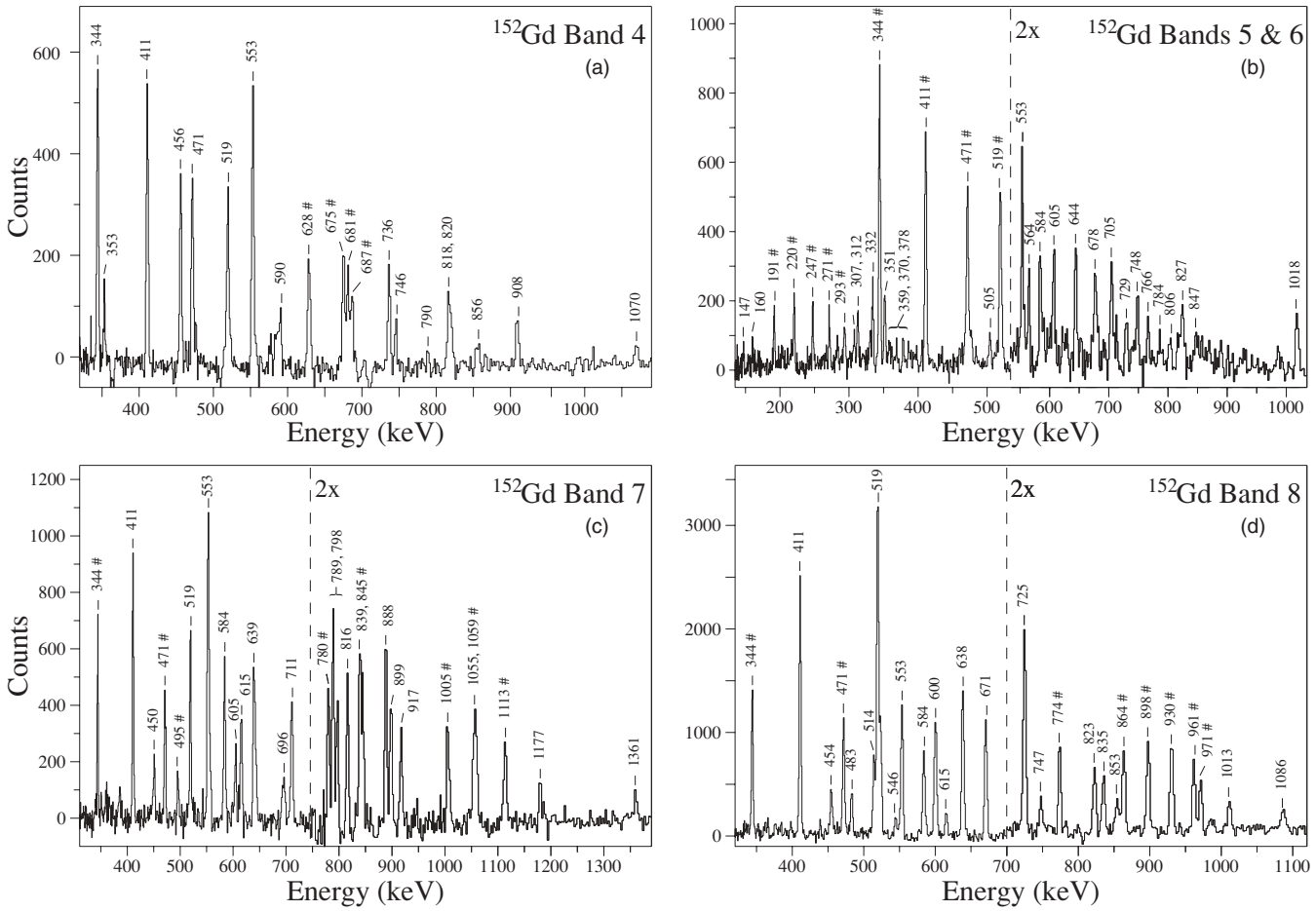

FIG. 2. Representative spectra for bands 4(a), 5(b), 6(b), 7(c) and 8(d) in ^{152}Gd. Peaks marked with a "#" symbol were included in the list of gates (see text for discussion) that produced each spectrum and may exhibit reduced intensity as a result. The dashed lines indicate an increase in scale to enhance the visibility of low-intensity, high-energy peaks.

multiple-transition gating lists were used extensively. The use of a gating list entailed creating separate gated spectra for each γ ray in the list, then combining them to generate a final spectrum. This technique produced spectra with little contamination, yet the significance of relative peak intensities was limited by the impact of including so many transitions in the gate. For example, to generate Fig. 2(c), three lists were used. The first list helped isolate the ^{152}Gd contribution and contained the 344- and 471-keV transitions. The second list focused on the most intense peaks in the band, 495, 780, and 845 keV, while the final list included the high spin transitions: 1005, 1055, 1059 and 1113 keV. The spectra generated by all iterations using one transition from each list were then combined in the final spectrum.

IV. DISCUSSION

Interpretation of the observed rotational bands in ^{152}Gd is based on a comparison with different configurations calculated in the Cranked Nilsson-Strutinsky (CNS) formalism [14–16]. Because pairing is neglected in these calculations, a quantitative comparison with experiment is only relevant in the high-spin region. In the calculations, different configurations are tracked and their evolution with increasing spin is followed. For each configuration at each spin value, the lowest energy in the $(\varepsilon_2, \gamma, \varepsilon_4)$ deformation space is found. In the low-lying configurations of ^{152}Gd, some valence protons are excited across the $Z = 64$ gap from the orbitals of $(d_{\frac{5}{2}}, g_{\frac{7}{2}})$ character to the $h_{\frac{11}{2}}$ orbitals while the valence neutrons are scattered over the orbitals of $(f_{\frac{7}{2}}, h_{\frac{9}{2}})$ and $i_{\frac{13}{2}}$ character. With the particle number fixed, it is then sufficient to label the configurations as $[\pi h_{\frac{11}{2}}, \nu i_{\frac{13}{2}}]$, where $\pi h_{\frac{11}{2}}$ represents the number of $h_{\frac{11}{2}}$ protons and $\nu i_{\frac{13}{2}}$ represents the number of $i_{\frac{13}{2}}$ neutrons. The energy is calculated as the sum of the smoothly varying rotating liquid drop energy and the shell energy. The former is based on the Lublin-Strasbourg drop (LSD) model [17] with the rigid body moment of inertia calculated from a mass distribution with a diffuse surface [16]. The shell energy is calculated from a modified oscillator potential [15] with the so called $A = 150$ single particle parameters [18]. Note that with the new developments described in Ref. [16], it is now possible to calculate absolute values of the energy. This is contrary to previous CNS calculations [14,15] where only relative energies could be compared.

The three bands of ^{152}Gd observed beyond $I = 30\hbar$ are plotted in Fig. 3(a) relative to a rotating liquid drop reference. The calculated configurations of the same parity and signature which are lowest in energy at $I \approx 40\hbar$ are plotted relative to the same reference in Fig. 3(b). This reference is calculated as the minimum in the $(\varepsilon_2, \gamma, \varepsilon_4)$-space of the rotating liquid drop energy using the same parameters as when calculating the total energy [16]. The I-dependence of this reference is similar but clearly not identical to our previous reference, $32.32A^{-\frac{5}{3}}I(I+1)$ MeV. With the present reference, the values E_{rld} are referred to as "microscopic energies" analogous to the microscopic energies in nuclear mass, see e.g. Ref. [19].

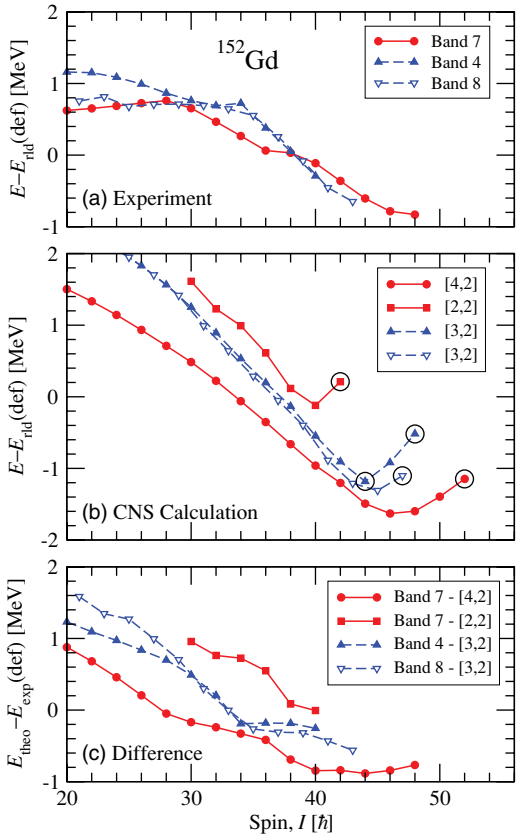

FIG. 3. (Color online) Excitation energy minus the rotating liquid drop energy, as defined in Ref. [16], plotted as a function of spin for bands 4, 7, and 8 in ^{152}Gd. (b) Theoretical behavior of configurations assigned to the higher-spin regions of the observed bands shown in panel (a). Also included is the [2,2] configuration which might be responsible for the uneven character of Band 7 in the $I = 30$–$40\hbar$ spin range. (c) Difference in energy between the observed bands shown in panel (a) and their theoretical counterparts shown in panel (b).

Considering the general agreement between calculations and experiment and the systematics of the high-spin bands in this region of nuclei, see e.g. Ref. [20], it appears safe to assign the [4,2] configuration to the positive parity band for $I > 40\hbar$ and to assign the [3,2] configuration to the negative parity bands for $I > 35\hbar$. The positive parity band is then observed two transitions short of the predicted termination at $I = 52\hbar$, which is built as $\pi(d_{\frac{5}{2}} g_{\frac{7}{2}})_{10}^{-4}(h_{\frac{11}{2}})_{16}^{4}\nu(h_{\frac{9}{2}} f_{\frac{7}{2}})_{14}^{4}(i_{\frac{13}{2}})_{12}^{2}$, where the subscripts indicate the spin contribution from the different groups of particles. Also, the negative parity bands are observed close to their terminating states. The difference compared with the positive parity state above is that only three protons are excited across the $Z = 64$ gap, $\pi(d_{\frac{5}{2}} g_{\frac{7}{2}})^{-3}(h_{\frac{11}{2}})^{3}$, with a maximum proton spin of $8.5 + 13.5 = 22\hbar$, but where also aligned states are formed at slightly lower spin values when the proton holes have a smaller contribution than their maximum value, $8.5\hbar$. In a similar way, also the $I = 48, 50\hbar$ states of the [4,2] configuration are very close to aligned in the sense that the calculated energy at oblate shape is not significantly higher (~100 keV) than at the shallow minimum

for triaxial shape. Therefore, the observed $I = 48\hbar$ state is probably very close to terminating or even terminating, i.e. aligned at oblate shape.

Going to somewhat lower spin values, the behavior displayed by the observed positive parity band, as in Fig. 3(a), is markedly different from the smooth evolution of the calculated [4,2] configuration, as in Fig. 3(b). This suggests that some other configuration mixes in for spin values below $I = 40\hbar$. This feature might be understood from a comparison with the isotone ^{154}Dy, see Ref. [20], where a configuration with only 2 $h_{\frac{11}{2}}$ protons is yrast for $I = 34, 36\hbar$. Therefore, the corresponding ^{152}Gd configuration, [2,2], is also drawn in Fig. 3(b). However, it turns out to be calculated approximately 1 MeV higher in energy than the [4,2] configuration. This becomes evident from Fig. 3(c), where the difference between the observed and calculated bands are drawn. For all the cases shown, this difference is within the expected accuracy of ± 1 MeV [16] which is another indication that we understand the high-spin bands of ^{152}Gd. The increasing difference between experiment and calculation with decreasing spin is as expected from the increasing importance of pairing correlations.

While we cannot expect to describe the absolute differences between calculations and experiment with a better accuracy than ± 1 MeV, one would expect the relative errors to be about the same for the different bands. In view of this, the displacement between the different curves in the Fig. 3(c) is somewhat surprising, i.e. the difference between experiment and calculations is about 0.5 MeV larger for the negative parity bands than for the positive parity band compared with the [4,2] configuration. Furthermore, if the positive parity band is compared with the [2,2] configuration, the difference curve is lifted by another 0.5 MeV. As the configurations differ by the number of protons excited across the $Z = 64$ gap, they would more or less overlap if this gap was increased by 0.5 MeV, i.e., if the $h_{\frac{11}{2}}$ shell was lifted by 0.5 MeV. In this context, it is interesting to compare with the early studies of terminating bands in this region. In the first calculations [21], the terminating states came at too high an energy relative to the more collective states in ^{158}Er and ^{154}Dy. It was then noted [22] that a quantitative agreement between calculations and experiment could be obtained if the $Z = 64$ gap was continuously increased when decreasing the number of valence protons outside the $^{146}_{64}$Gd$_{82}$ doubly-closed nucleus. It was also concluded that an increase of approximately 500 keV relative to the value used for the well-deformed rare-earth nuclei [23] was appropriate for $A = 154$–158 (8–12 valence nucleons). This increase of the $Z = 64$ gap was later formalized by introducing the so-called $A = 150$ parameters [18] used here. Now, with even fewer valence nucleons in ^{152}Gd, it turns out that another increase of the gap by approximately 500 keV (i.e., an increase of the $h_{\frac{11}{2}}$ shell by $\sim$1 MeV relative to the position originally used for the deformed rare-earth nuclei) appears to improve the agreement between calculations and experiment. This is thus consistent with the conclusion of Ref. [22] that the (effective) $Z = 64$ gap increases when approaching the $^{146}_{64}$Gd$_{82}$ doubly-closed nucleus.

For negative parity, the calculated [3,2] bands are smooth in the spin range $I \approx 25$–$43\hbar$ while the observed bands show some discontinuity and a band crossing at $I \approx 34\hbar$. In the calculations, other configurations, like [4,1] and at lower spin values [5,2] cross the [3,2] bands. Indeed, with the parameters used in the calculations, the [4,1] bands are yrast up to $I \approx 38\hbar$ which seems inconsistent with experiment. However, with the increase of the $Z = 64$ gap discussed above, this crossing would come at a lower spin value and be more consistent with experiment. This increased agreement must be tempered with the fact that it is difficult to draw definitive conclusions below $I \approx 35\hbar$ due to the increasing importance of pairing.

As exploited for the high-spin states above, it is instructive to consider $^{146}_{64}$Gd$_{82}$ as a spherical "core" when discussing valence nucleons. Going to lower spin values, the addition of particles or holes beyond the core typically has a significant impact on nuclear behavior. Surprisingly, the addition of 2 protons to $^{152}_{64}$Gd$_{88}$, most likely in the $[411]_{\frac{3}{2}}$ orbital, seems to have remarkably little impact on the characteristics of $^{154}_{66}$Dy$_{88}$ [12]. In contrast to this observation, the removal of 2 protons from ^{152}Gd, creating ^{150}Sm, or the addition of 2 protons to ^{154}Dy, producing ^{156}Er, significantly alters the observed behavior. These changes in the $N = 88$ isotones as a function of proton number are illustrated in Fig. 4, where the deviation in energy from a reference, the yrast band of ^{154}Dy, is plotted for the yrast bands of $N = 88$ transitional nuclei. Notice the remarkable similarity between the γ-ray energies of the yrast bands of ^{152}Gd and ^{154}Dy [12], which is on the order of a few keV up to $\sim$700 keV and $\sim 20\hbar$, i.e. $\lesssim 1\%$. This situation between ^{152}Gd and ^{154}Dy is a rare occurrence of almost identical γ-ray fingerprints for two different nuclei. Indeed, in the calculations of Ref. [24], the ground state deformations of ^{152}Gd ($\beta \approx 0.205$) and ^{154}Dy ($\beta \approx 0.198$) are predicted to be very similar, whereas the values for the other $N = 88$ isotones, apart from ^{150}Sm ($\beta \approx 0.198$), are markedly different: ^{156}Er ($\beta \approx 0.182$), ^{158}Yb($\beta \approx 0.167$), and ^{160}Hf ($\beta \approx 0.141$). It should be noted that a similar situation

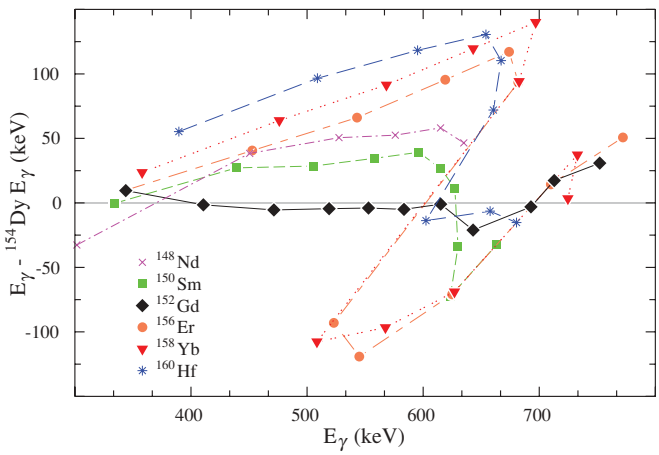

FIG. 4. (Color online) Comparison of yrast γ-ray energies for several $N = 88$ isotones. The transitions in ^{154}Dy are used as a reference and subtracted from the corresponding γ rays in each isotone. Thus, ^{154}Dy forms the line at zero. Note the great similarity between ^{152}Gd and ^{154}Dy. The discontinuities above 600 keV correspond to the first $i_{\frac{13}{2}}$ neutron backbend in these nuclei.

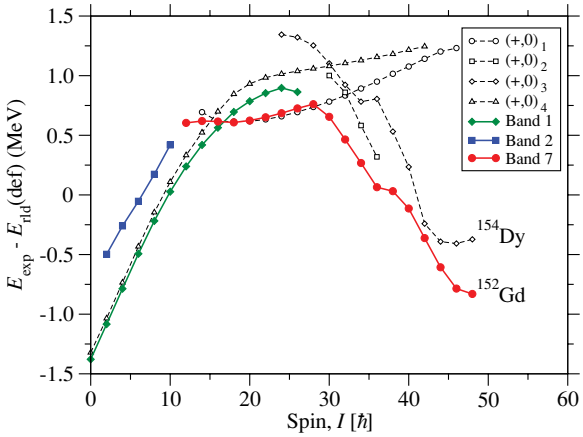

FIG. 5. (Color online) Excitation energy minus the rotating liquid drop energy, as defined in Ref. [16], shown as a function of spin for observed high-spin positive-parity states in ^{152}Gd, full lines and filled symbols, and ^{154}Dy, dashed lines and open symbols. Note how Band 7 in ^{152}Gd follows the lower energy states in the three $(+,0)_1$, $(+,0)_2$ and $(+,0)_1$ bands of ^{154}Dy, supporting the present interpretation of ^{152}Gd.

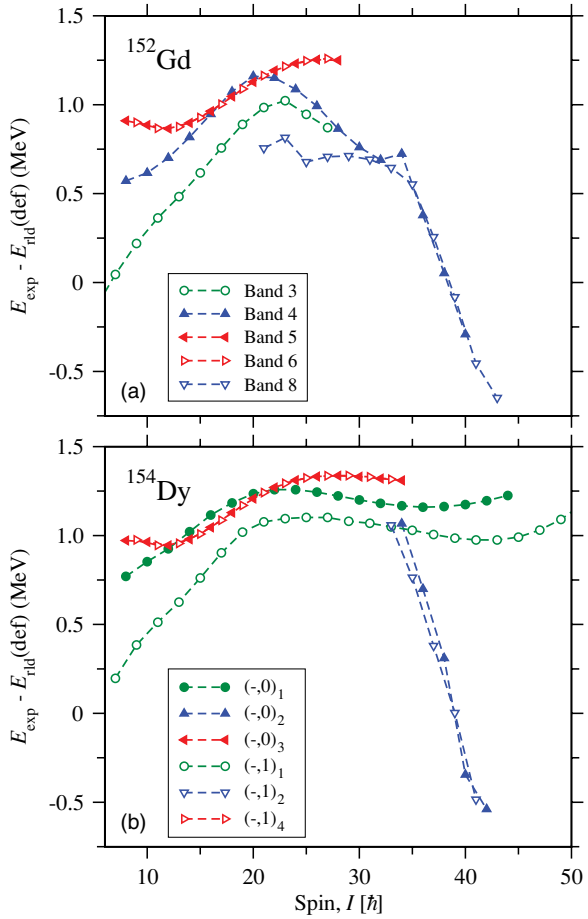

FIG. 6. (Color online) Excitation energy minus the rotating liquid drop energy, as defined in Ref. [16], for the negative parity bands in ^{152}Gd and ^{154}Dy illustrating the similarities between these two nuclei.

was pointed out in Ref. [3] concerning γ-ray transitions in the $N = 89$ isotones ^{153}Gd and ^{155}Dy.

Considering the large similarities between the low- and intermediate-spin yrast states of ^{154}Dy and ^{152}Gd, it is interesting to compare their spectra in the full spin range. This is done for the positive parity, even spin states in Fig. 5. The figure suggests that band 7 of ^{152}Gd can be identified with three different structures in ^{154}Dy, namely $(+,0)_1$, $(+,0)_2$, and $(+,0)_3$ [20]. While the $(+,0)_1$ band remains rotational in nature to high spin, the corresponding structure is not observed in ^{152}Gd after a spin of $28\hbar$. In ^{154}Dy the downward sloping band which culminates in the favored terminating $36^+\hbar$ state corresponds to the $(+,0)_2$ band and was assigned the configuration of [2,2] [20]. This terminating state corresponds to the maximal alignment of the $\pi(h_{\frac{11}{2}})^2_{10^+}\nu[(f_{\frac{7}{2}})^2(h_{\frac{9}{2}})^2(i_{\frac{13}{2}})^2]_{26^+}$ configuration [22]. As discussed above, this supports the assignment of the [2,2] configuration to this section of Band 7 in ^{152}Gd. The $(+,0)_3$ band in ^{154}Dy terminates near spin 46 or $48\hbar$, and has been assigned a configuration of [4,2] which again is consistent with the [4,2] assignment for the high spin section of Band 7 in ^{152}Gd. The figure indicates that the $I \geqslant 28\hbar$ portion of Band 7 can be seen as a continuation of Band 1 suggesting that in future experiments, one should look for transitions decaying from the two 28^+ states associated with Band 7 to the top 26^+ state of Band 1.

As can be seen in Fig. 6, the similarity between the two nuclei extends to the negative parity bands as well. In the spin $I = 10$–$30\hbar$ range, the strongly coupled bands, Band 5, 6 and $(-,0)_3$ and $(-,1)_4$, respectively, are almost identical when plotted relative to the rotating liquid drop energy. It is also clear that the low-spin ranges of bands 3 and 4 in ^{152}Gd should be identified with the $(-,1)_1$ and $(-,0)_1$ bands in ^{154}Dy. These bands all display a change in curvature above $I = 20\hbar$ indicating a common bandcrossing, although the change in slope is slightly greater in ^{152}Gd. In the $I = 22$–$35\hbar$ spin range a new band, Band 8, is present in ^{152}Gd which lacks a corresponding partner in ^{154}Dy. However, through band crossings near $I = 35\hbar$ in this band and Band 4, down-sloping structures are created which show similar features as the $(-,0)_2$ and $(-,1)_2$ structures in ^{154}Dy. This similarity supports the adjustment of previously reported spin and parity values for Band 4 [11,12] and it also supports that the [3,2] configuration is assigned to these high-spin bands in the respective nuclei.

The coexistence of structures at high spin in ^{154}Dy is evident from the vastly different trajectories of the bands plotted in Fig. 5. These different slopes are attributed to different and evolving nuclear shapes [20,22]. The negatively sloped segments are associated with weakly collective structures evolving toward termination while positive slopes are characteristic of prolate collective rotation. Though only the more favored states are observed, the current work clearly indicates the occurrence of a shape change in the high-spin bands of ^{152}Gd similar to that documented in ^{154}Dy. Supporting this, theory calculations for each of the assigned configurations indicate a migration across the gamma plane toward oblate deformation (and termination) at high spin in ^{152}Gd.

While the high-spin behavior of the three lowest energy bands in ^{152}Gd has been the main focus of this work, it is interesting to extend this comparison to the other sequences

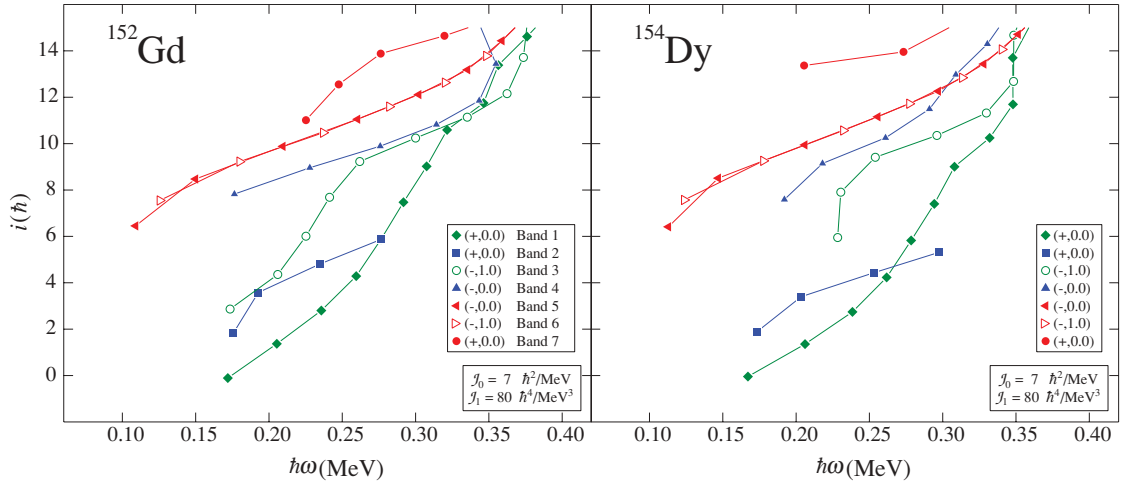

FIG. 7. (Color online) Experimental alignment (i) plotted as a function of rotational frequency ($\hbar\omega$) for bands in ^{152}Gd and ^{154}Dy illustrating the fact that strong similarities extend to low spin values for all configurations.

observed in ^{152}Gd. When considering lower spin values, alignment plots are often very useful. Therefore experimental alignments (i) of all the bands in ^{152}Gd are plotted as a function of rotational frequency in Fig. 7 along with their counterparts in ^{154}Dy. This is done for rotational frequencies up to $\hbar\omega \approx 0.35$ MeV corresponding to spin values up to or slightly beyond $I = 20\hbar$. Once again, even when plotting such a sensitive quantity, strong similarities are observed. Going one step further, measurements of the B(M1)/B(E2) branching ratios for bands 5 and 6 in ^{152}Gd overlap, within uncertainties, those of the equivalent $(-,0)_3$ and $(-,1)_4$ bands in ^{154}Dy. This indicates that the configurations of the corresponding bands are the same, $\nu[(i_{\frac{13}{2}})^1 \otimes (h_{\frac{11}{2}})^{-1}]$, and that their deformations are very similar.

V. CONCLUSIONS

An examination of the high-spin characteristics of ^{152}Gd has been conducted and significant additions have been made to the previously reported level scheme. Configuration assignments have been proposed based on Cranked Nilsson-Strutinsky calculations for the three bands which reach high spin ($\sim 40\hbar$). It appears that a better agreement between calculations and experiment is obtained if the $Z = 64$ shell gap increases with a decreasing number of valence particles outside the doubly-closed $^{146}_{64}Gd_{82}$ nucleus. A remarkable similarity, not only in behavior, but also in γ-ray transition energies between ^{152}Gd and ^{154}Dy was reported. This similarity supports the conclusion of an observed angular momentum induced shape change in ^{152}Gd from prolate collective rotation toward oblate non-collective behavior via the mechanism of band termination above spin $30\hbar$.

ACKNOWLEDGMENTS

Discussions with J.F. Sharpey-Schafer are gratefully acknowledged. The authors would like to extend special recognition to David Radford for his valuable aid and indispensable RADWARE software. Support for this work was provided by the National Science Foundation, the State of Florida, the U.S. Department of Energy Office of Nuclear Physics, through contract No. DE-AC02-06CH11357 (Argonne National Laboratory), the Department of Energy by University of California Lawrence Livermore National Laboratory under contract W-7405-Eng-48, the UK Engineering and Physical Sciences Research Council and the Swedish Science Research Council.

[1] I. Ragnarsson, A. Sobiczewski, R. K. Sheline, S. E. Larsson, and B. Nerlo-Pomorska, Nucl. Phys. **A233**, 329 (1974).
[2] R. F. Casten, D. D. Warner, D. S. Brenner, and R. L. Gill, Phys. Rev. Lett. **47**, 1433 (1981).
[3] T. B. Brown, M. A. Riley, D. Campbell, D. J. Hartley, F. G. Kondev, J. Pfohl, R. V. F. Janssens, S. M. Fischer, D. Nisius, P. Fallon, W. C. Ma, J. Simpson, and J. F. Sharpey-Schafer, Phys. Rev. C **66**, 064320 (2002).
[4] R. V. F. Janssens and F. Stephens, Nucl. Phys. News **6**, 9 (1996).
[5] F. G. Kondev, M. A. Riley, R. V. F. Janssens, J. Simpson, A. V. Afanasjev, I. Ragnarsson, I. Ahmad, D. J. Blumenthal, T. B. Brown, M. P. Carpenter, P. Fallon, S. M. Fischer, G. Hackman, D. J. Hartley, C. A. Kalfas, T. L. Khoo, T. Lauritsen, W. C. Ma, D. Nisius, J. F. Sharpey-Schafer, and P. G. Varmette, Phys. Lett. **B437**, 35 (1998).
[6] D. C. Radford, Nucl. Instrum. Methods A **361**, 297 (1995).
[7] M. Cromaz, Nucl. Instrum. Methods A **462**, 519 (2001).
[8] A. Kramer-Flecken, T. Morek, R. M. Lieder, W. Gast, G. Hebbinghaus, H. M. Jager, and W. Urban, Nucl. Instrum. Methods A **275**, 333 (1989).
[9] L. P. Ekstrom and A. Nordlund, Nucl. Instrum. Methods A **313**, 421 (1992).
[10] D. B. Campbell, Ph.D. Thesis, Florida State University, 2004.
[11] D. R. Zolnowski, M. B. Hughes, J. Hunt, and T. T. Sugihara, Phys. Rev. C **21**, 2556 (1980).

[12] S. Wang, H. Hua, J. Meng, Z. H. Li, S. Q. Zhang, F. R. Xu, H. L. Liu, Y. L. Ye, D. X. Jiang, T. Zheng, Q. J. Wang, Z. Q. Chen, C. E. Wu, G. L. Zhang, D. Y. Pang, J. Wang, J. L. Lou, B. Guo, G. Jin, S. G. Zhou, L. H. Zhu, X. G. Wu, G. S. Li, S. X. Wen, C. Y. He, X. Z. Cui, and Y. Liu, Phys. Rev. C **72**, 024317 (2005).

[13] J. F. Sharpey-Schafer, S. M. Mullins, R. A. Bark, E. Gueorguieva, J. Kau, F. Komati, J. J. Lawrie, P. Maine, A. Minkova, S. H. T. Murray, N. J. Ncapayi, and P. Vymers, Proc. XLIV Int. Winter Meeting on Nuclear Physics, Bormio, Italy, January 29–February 5, 2006, p. 295.

[14] A. V. Afanasjev, D. B. Fossan, G. J. Lane, and I. Ragnarsson, Phys. Rep. **322**, 1 (1999).

[15] T. Bengtsson and I. Ragnarsson, Nucl. Phys. **A436**, 14 (1985).

[16] B. G. Carlsson and I. Ragnarsson, Phys. Rev. C **74**, 011302(R) (2006).

[17] K. Pomorski and J. Dudek, Phys. Rev. C **67**, 044316 (2003).

[18] T. Bengtsson, Nucl. Phys. **A512**, 124 (1990).

[19] P. Möller, J. R. Nix, W. D. Myers, and W. J. Swiatecki, At. Data Nucl. Data Tables **59**, 185 (1995).

[20] W. C. Ma, R. V. F. Janssens, T. L. Khoo, I. Ragnarsson, M. A. Riley, M. P. Carpenter, J. R. Terry, J. P. Zhang, I. Ahmad, P. Bhattacharyya, P. J. Daly, S. M. Fischer, J. H. Hamilton, T. Lauritsen, D. T. Nisius, A. V. Ramayya, R. K. Vadapalli, P. G. Varmette, J. W. Watson, C. T. Zhang, and S. J. Zhu, Phys. Rev. C **65**, 034312 (2002).

[21] T. Bengtsson and I. Ragnarsson, Phys. Scr. **T5**, 165 (1983).

[22] H. W. Cranmer-Gordon, P. D. Forsyth, D. V. Elenkov, D. Howe, J. F. Sharpey-Schafer, M. A. Riley, G. Sletten, J. Simpson, I. Ragnarsson, Z. Xing, and T. Bengtsson, Nucl. Phys. **A465**, 506 (1987).

[23] S. G. Nilsson, C. F. Tsang, A. Sobiczewski, Z. Szymanski, S. Wycech, C. Gustafson, I. L. Lamm, P. Moller, and B. Nilsson, Nucl. Phys. **A131**, 1 (1969).

[24] W. Nazarewicz, M. A. Riley, and J. D. Garrett, Nucl. Phys. **A512**, 61 (1990).